Laser and Particle Beams (2001), *19*, 169–173. Printed in the USA.

ICF target ignition studies in planar, cylindrical, and spherical geometries

A. DJAOUI

Rutherford Appleton Laboratory, Chilton, Didcot, Oxon OX11 0QX, United Kingdom

(Received 30 November 2000; ACCEPTED 5 February 2001)

Abstract

A model for nonlocal α particle transport is implemented in a one-dimensional radiation hydrodynamics code and applied for typical directly and indirectly driven ICF target simulations. Ignition criteria are compared for four configurations; spherical, cylindrical, planar with a central hot spot, and another planar configuration with a hot spot on one side. This last planar configuration is then used for fast ignitor studies, since it is able to simulate hot spot formation by direct laser heating and free expansion towards the incoming beam. Ignition requirements as a function of laser intensity and pulse length, taking into account the relationship between intensity, hot electron temperature, and range, are then determined.

1. INTRODUCTION

Models for energy gain of idealized spherical configurations of Inertial Confinement Fusion (ICF) targets have been extensively studied for isobaric (Meyer-ter-Vehn, 1982) as well as isochoric (Atzeni, 1995) configurations. The isobaric case with a central hot spot is considered to be a good representation of the final stages of the implosion of hollow shells in conventional directly and indirectly driven ICF studies. The isochoric case is more appropriate for the fast ignitor concept (Tabak *et al.*, 1994), where rapid heating of a precompressed core occurs on time scales smaller than hydrodynamic time scales. These configurations are suitably modeled with one-dimensional codes in spherical geometry. Spherical geometry, however, is only a rough approximation for the heating phase of the fast ignitor where a hot spot is directly created by an intense laser beam on the edge of the compressed core. In this case, a burn wave propagates into the dense core away from the incoming laser while hydrodynamics free expansion proceeds towards the beam. Within the limits of a one-dimensional code, it is more appropriate to model the situation in planar geometry, where both burn propagation and expansion are modeled. Interpretation of results in planar geometry and their relationship to the conventional spherical and cylindrical geometry results are presented in this work.

Address correspondence and reprint requests to: Dr. A. Djaoui, R2, 3.15, Rutherford Appleton Laboratory, Chilton, Didcot, OXON, OX11 0QX, United Kingdom. E-mail: a.djauoi@rl.ac.uk.

Since thermonuclear α particle transport plays an important role in the burn wave dynamics, we compare a nonlocal to a local α particle energy deposition model for typical directly and indirectly driven ICF targets. To illustrate the effect of geometry on the ignition condition, we compare ignition conditions for different geometries. Further calculations for the fast ignitor are carried out using a planar target irradiated on one side. A model for the hot electron energy deposition is implemented. We relate the hot electron temperature to the incident laser intensity through a well-known relation. We look into the intensity/pulse length requirements for ignition for a given conversion efficiency of laser to hot electrons and a given hot electron spectrum.

2. CHARGE PARTICLE TRANSPORT EFFECTS ON DIRECTLY AND INDIRECTLY DRIVEN TARGETS

First we look at effect of α particle transport on directly (laser irradiation) and indirectly (X-ray irradiation) driven ICF targets. The simulations are performed with a 1D Lagrangian radiation-hydrodynamic code (Christiansen *et al.*, 1974; Djaoui, 1995), where the coupled equation of motion and energy equations for ions and free electrons are solved, taking into account heat conduction, electron-ion energy exchange, multigroup radiative energy transfer, and thermonuclear burn. To simulate thermonuclear burn wave propagation, a good description of α particle transport is needed. Nonlocal transport of α particles from the DT fusion is implemented assuming isotropic emission and straight paths.

https://doi.org/10.1017/S0263034601191275 Published online by Cambridge University Press

As the α particles traverse a given path length they lose their energy to electrons and ions according to a standard energy loss formula (Fraley *et al.*, 1974; Lindl, 1995). Particles reaching the boundary of the target are lost. The fraction of α particle energy transferred to ions depends on its energy as well as the plasma temperature. A particle with an initial energy E_α (in megaelectronvolts), transfers a fraction f_i to ions as approximated by the simple formula

$$f_i = \frac{1}{1 + (E_\alpha/3.5)(32/T_e)},$$

T_e being the electron temperature in kiloelectronvolts. This is compared in Figure 1 to more detailed calculations of energy losses to electrons and ions (Fraley *et al.*, 1974; Lindl, 1995). For the temperatures shown, the fractional energy transferred to the ions is almost independent of density and increases as α particle energy is reduced below 3.5 MeV.

Simulations with local and nonlocal energy deposition were performed for two targets which consist of a solid DT shell filled with DT gas and surrounded with a plastic (CH) ablator. For the directly driven target with an initial outside radius of 1.765 mm and a shaped driving laser pulse with a maximum power of 40 TW, no significant difference in target performance was found with local and with nonlocal α particle transport. This was not the case for the indirectly driven NIF target (Djaoui, 1996) with an outside radius of 1.11 mm and a maximum X-ray radiation temperature drive of about 300 eV. Figure 2 shows the effect of nonlocal α particle transport on thermonuclear energy yield as a function of maximum temperature. With nonlocal transport, the ignition window is shifted to higher temperature as well as being narrower than the case with local transport.

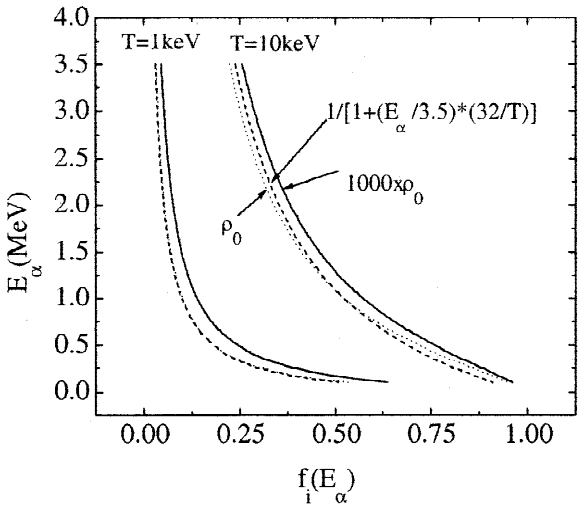

Fig. 1. Fractional energy transfer to ions as a function of initial α particle energy for two plasma temperatures (1 keV and 10 keV). The simple formula (dashed curves) fits the detailed calculations well at solid density (dotted curves) and at a thousand times solid (continuous curves).

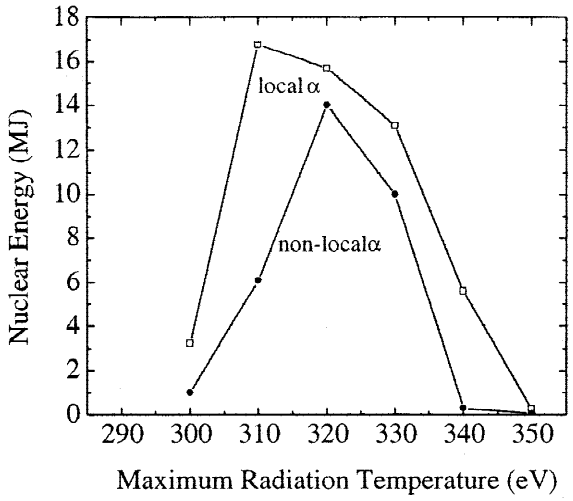

Fig. 2. Thermonuclear energy yield as a function of maximum X-ray drive temperature for the NIF target as calculated with local and nonlocal α particle energy deposition.

3. IGNITION CURVES FOR SIMPLE CONFIGURATIONS

A large number of simulations of ignition and burn performance for the four simple configurations described above are performed. For these calculations, a DT target which is a thousand times compressed with an initial density of 250 g/cm^3 and an initial ρr thickness of 4.2 g/cm^2 (in addition to a hot spot) is used. The size of a hot spot with equal electron (T_e) and ion (T_i) temperatures is increased until ignition and high gain are obtained. Figure 3 shows

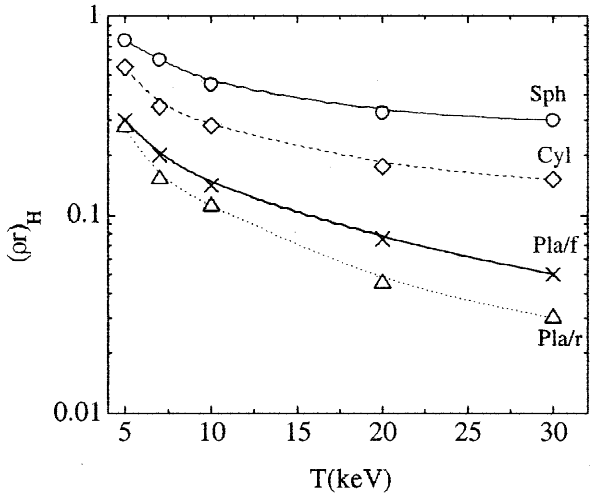

Fig. 3. Ignition boundary in $(\rho r)_H - T$ plane. Curves for configurations with a central hot spot are shown. These are spherical (Sph), cylindrical (Cyl), and planar with a reflecting boundary (Pla/r) corresponding to the center of the hot spot. A fourth configuration, planar with a free boundary (Pla/f), has a hot spot next to that boundary. The $(\rho r)_H$ shown for the planar cases represents half the total thickness of the hot spot.

https://doi.org/10.1017/S0263034601191275 Published online by Cambridge University Press

such curves for spherical, cylindrical, and planar configurations with a central hot spot. These cases are modeled with a reflecting left boundary condition which corresponds to the center of the hot spot. Therefore, for the planar case, $(\rho r)_H$ refers to half the thickness of the hot spot. The results for a fourth configuration (planar with a free left boundary condition) are also shown. Here the quoted $(\rho r)_H$ also refers to half the total thickness.

The results for spherical geometry are similar to Atzeni's (1995) isochoric spherical case. As the geometry is changed to cylindrical and then to planar, less stringent $(\rho r)_H$ requirements are needed for ignition at a given temperature. This is mainly because of reduced energy losses from the hot spot in these geometries. The planar case is infinite in two dimensions and only experiences heat and expansion losses in one direction. The cylindrical case is infinite in one dimension and therefore only has losses in two directions. The spherical case, however is subject to losses in the three spatial directions. For the values of the initial hot spot temperatures shown, the results for the fourth configuration are slightly higher than the planar reflecting case. For the planar case, allowing for free expansion of the hot spot has increased the requirements for ignition only slightly at low temperatures but almost a factor of two at the higher temperatures.

In the fast ignitor concept the laser-produced hot electrons deposit their energy preferentially to the background plasma electrons and this results initially in a much higher electron temperature than the ion temperature. Ions are then heated to fusion temperature through electron–ion energy exchanges. It is, however, important that this energy exchange occurs before any significant losses from the electrons (heat conduction, radiation, and expansion) occur. To test this, we compare in Figure 4 the result for the fourth configuration (Pla/f) with two different initial conditions. Here the total $(\rho r)_H$ thickness is plotted against the sum of the electron and ion temperatures. The first curve ($T_e = T_i$) corresponds to the equal electron and ion temperature, and the second ($T_e \gg T_i$) corresponds to an electron temperature much higher than the ion temperature. It is seen that with all energy initially put mainly into the electrons, only a slight increase $(\rho r)_H$ is needed for ignition to occur for a given $(T_e + T_i)$. Under these conditions, efficient energy exchange ensures that almost equal electron and ion temperatures are rapidly reached before significant losses occur.

For a planar DT target, the amount of energy needed to heat a hot spot with a given ρr to temperatures T_e and T_i is given by $E(\mathrm{J/cm^2}) = 5.76 \times 10^7\, \rho r(T_e + T_i)$, where T_e and T_i are in kiloelectronvolts. Four contours of constant energy input (2×10^8, 3×10^8, 4×10^8, and 5×10^8 J/cm^2) are shown in Figure 4. The ignition condition for the planar reflecting configuration (Pla/r) with $T_e = T_i$ is also shown and lies just above the contour for 2×10^8 J/cm^2 at all initial temperatures. The requirements for the configuration of interest to the fast ignitor (Pla/f) with $T_e \gg T_i$ are nearer the contour for 4×10^8 J/cm^2. This is about twice the requirement for the planar reflecting configuration (Pla/r) with $T_e = T_i$. A similar increase in energy requirements is expected for a cylindrical or spherical hot spot when all the energy is dumped into electrons when and only when the hot spot is created on the edge of the target rather than at the center.

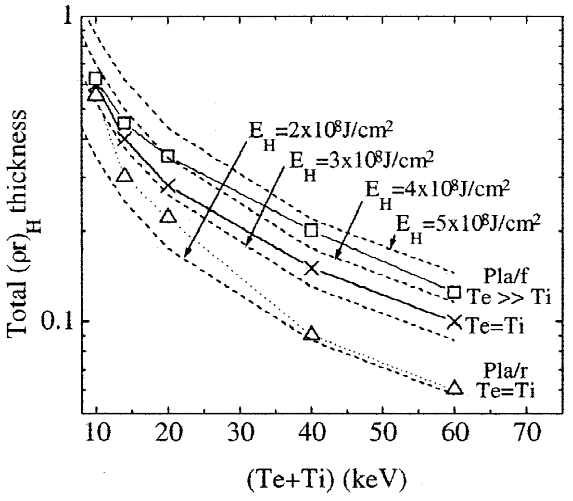

Fig. 4. Ignition boundary for planar configurations with hot spot on one side (Pla/f) with $T_e = T_i$ (crosses) and $Te \gg Ti$ (squares). The planar case with a central hot spot (Pla/r) is also shown (triangles) for comparison. Four contours (dashed lines) for energy input of 2×10^8 J/cm^2, 3×10^8 J/cm^2, 4×10^8 J/cm^2 and 5×10^8 J/cm^2 are superimposed on the ignition curves. The $(\rho r)_H$ corresponds to the total thickness of the hot spot.

From Figure 3, at 10 keV a $(\rho r)_H$ of 0.5 g/cm^2 is required in spherical geometry corresponding to an energy input of 9.6 kJ. The total $(\rho r)_H$ for the planar case is 0.22 (see Fig. 4) with an energy requirement of about 2.5×10^8 J/cm^2. Taking a planar slab with the same mass as the sphere would require an area of 3.8×10^{-5} cm^2 and a corresponding energy input of 9.5 kJ. Using the same argument for the planar case with free boundary (Pla/f), an energy input requirement of 15 kJ is found. Two-dimensional calculations (Atzeni, 1999) show minimum ignition energy of between 13 kJ and 20 kJ, slightly up from the 9.6 kJ of the spherical ideal configuration, and in rough agreement with the planar case with a free boundary. This illustrates that the planar configuration (Pla/f) with a hot spot at one side is a useful model for rapid simulations of the fast ignitor physics.

Ignition requirements in planar geometry are given per unit area and are independent of density. In cylindrical geometry, a requirement of about 1 MJ/cm can easily be worked out with the help of the results in Figure 3. This is expressed as energy per unit length and scales as ρ^{-1} as a result the mass scaling with density for a given ρr in cylindrical geometry. It is well known that in spherical geometry the scaling goes as ρ^{-2}.

https://doi.org/10.1017/S0263034601191275 Published online by Cambridge University Press

4. INTENSITY/PULSE LENGTH REQUIREMENTS

In the 2D calculation by Atzeni (1999), the hot electron energy/range dependence on the intensity was not explicitly taken into account. The validity is therefore limited to intensities which generate hot electrons with penetration depths comparable to that used in his study. Simulations (Wilks, 1993) have shown that the hot electron spectrum can be represented with a Maxwellian with a temperature given by

$$kT\,(\mathrm{MeV}) = 0.511 \times \left[\sqrt{1 + \frac{I\lambda^2}{1.4 \times 10^{18}}} - 1\right],$$

where I is the incident laser intensity in Watts per centimeter squared and λ, the wavelength in microns. Hot electrons slow down by losing energy to the background thermal electrons while being deflected by background ions. The continuous slowing-down range and penetration depth were calculated by Deutsch *et al.* (1996). A good fit to the penetration depth in grams per centimeter squared as a function of energy E in kiloelectronvolts is given by $(\rho r)_e = 6.7 \times 10^{-5} E^{1.2}$.

Planar geometry makes studies of intensity/pulse length relatively easy if the conversion efficiency from laser energy to forwardly directed hot electrons is assumed known. For the hot electron energy transport and deposition, a multigroup treatment of the Maxwellian distribution is implemented. The energy loss formula is scaled so as to recover the penetration depth as a function of energy as calculated by Deutsch *et al.* (1996). Figure 5 shows target gain as a function of laser pulse length for three different incident intensities, having a wavelength of 1 μm. The pulse is constant in time and a conversion efficiency into hot electron of one is assumed.

At 10^{19} W/cm^2, the hot electron temperature is 0.95 MeV with typical penetration depths of $(\rho r)_e = 0.3$ g/cm^2. This is much smaller than the total target thickness of 4.5 g/cm^2, and results in all electrons depositing their energy within the target. At 10^{20} W/cm^2, the temperatures is 3.8 MeV while at 10^{21} W/cm^2 it is 13.1 MeV. For these cases, electrons in the tail of the distribution are able to escape if they have a range longer than the target size. In all three cases, the gain decreases linearly as the pulse length is increased beyond the minimum pulse for maximum gain. The effect of decreasing the conversion efficiency from laser to hot electrons is shown for the 10^{20} W/cm^2.

Figure 6 shows the pulse length and the input and absorbed energies required for ignition as a function of intensity, for a conversion efficiency from laser to hot electrons η_L of 50%. At the lowest intensity shown (10^{19} W/cm^2), the pulse length requirement is at 290 ps and the absorbed energy requirement is 1.45×10^9 W/cm^2. As the intensity increases, the hot electron temperature increases and consequently the penetration depth of electrons in the high energy tail becomes larger than the target thickness. This results in higher energy input requirements, but the absorbed energy input requirement is constant at a level equal to 1.1×10^9 W/cm^2. This is despite the fact that density and temperature profiles are quite different for low- and high-intensity cases. For the low-intensity, long-pulse case, expansion and shock-wave compression result in a hot expanded region towards the laser and the rest of the target compressed to about twice the initial density. The hot electrons having a short range mainly heat a small spot on the surface of the target, but by the time the laser pulse is switched off, the rest of the target is also heated by conduction. For the high-intensity, short-

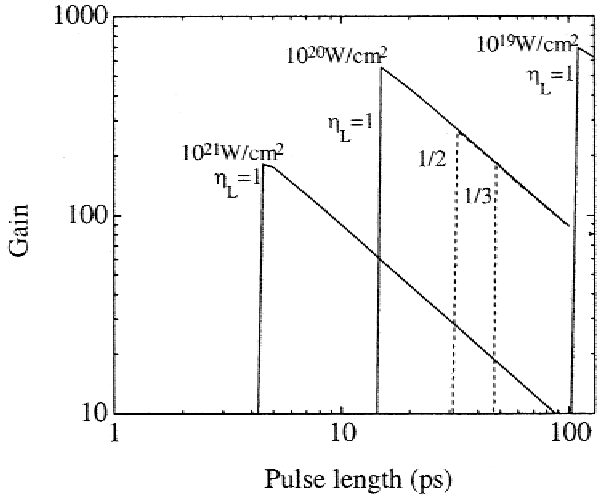

Fig. 5. Target thermonuclear gain as a function of pulse length for three laser intensities, 10^{19} W/cm^2, 10^{20} W/cm^2, and 10^{21} W/cm^2, and a conversion efficiency from laser to forward-going hot electrons η_L of 1. For 10^{20} W/cm^2, the curves for conversion efficiencies $\eta_L = \frac{1}{2}$ and $\eta_L = \frac{1}{3}$ are also shown.

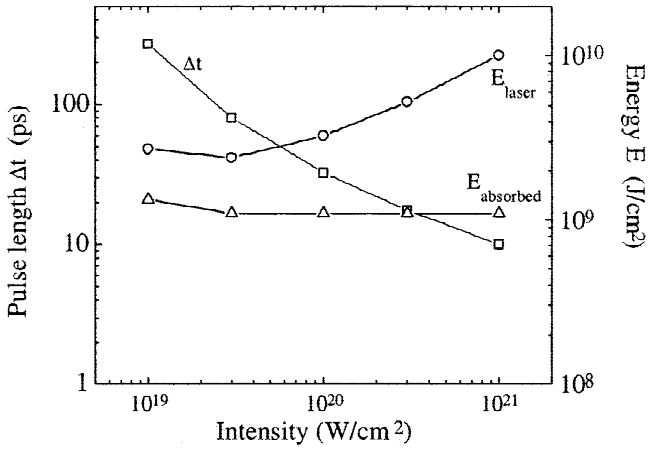

Fig. 6. Laser pulse length Δt, input, and absorbed energy required for ignition as a function of incident intensity. The laser wavelength is 1 μm and a conversion efficiency into forward-going hot electron of 50% is assumed.

https://doi.org/10.1017/S0263034601191275 Published online by Cambridge University Press

pulse case, hydrodynamic effects are not in evidence, and the density is almost constant at the initial value. The target is also fairly uniformly heated as in the long-pulse case, but this time, it is due to the long range of the hot electrons, not heat conduction. The fact that both cases show features at the end of the heating pulse that are characteristic of a volume heated configurations partly explains the requirement of an almost constant absorbed energy, independent of intensity/pulse length.

5. CONCLUSION

A model for thermonuclear α particle transport in ICF targets is implemented in a one-dimensional radiation hydrodynamics code, and is shown to affect results for the indirectly driven NIF target. Ignition criteria for 1D spherical, cylindrical, and planar geometry isochoric configurations with a central hot spot as well as planar geometry with a hot spot on one side are shown. It is found that in planar geometry, an energy input of about 4×10^8 J/cm^2 is needed. For a spherical configuration at a density of 250 g/cm^3, the requirement is 9.6 kJ. Although the criteria in $\rho r - T$ space are quite different, energy requirement for ignition are of the same order when comparing requirements for equal masses of fuel in spherical and planar geometry. This weak dependence on geometry allows us to take advantage of the simplicity of planar geometry for fast ignitor studies, using the ideal configuration results presented in this work as a reference.

The interaction of a constant power laser beam with a planar target is simulated, while taking into account the details of hot electron energy depositions, and the intensity range relationship. Assuming the conversion efficiency from laser energy to forward traveling hot electrons is known, criteria for ignition in terms of energy per unit area are calculated. Allowing for finite pulses and less than optimal energy deposition results in increased energy requirements up to 1.45×10^9 J/cm^2 as compared to the corresponding ideal hot spot configuration requirement of 4×10^8 J/cm^2.

REFERENCES

Atzeni, S. (1995). *J. Appl. Phys.* **34**, 1980.

Atzeni, S. (1999). *Phys. Plasmas* **6**, 3316.

Christiansen, J.P., Ashby, D.E.T.F. & Roberts, K.V. (1974). *Computer Phys. Commun.* **7**, 271.

Deutsch, C., Furukawa, H., Mima, K., Murakami, M. & Nishihara, K. (1996). *Phys. Rev. Lett.* **17**, 2483.

Djaoui, A. (1995). *J. Quant. Spectrosc. Radiat. Transfer* **54**, 143.

Djaoui, A. (1996). *Phys. Plasmas* **3**, 4677.

Fraley, G.S., Linnebur, E.J., Mason, R.J. & Morse, R.L. (1974). *Phys. Fluids* **17**, 474.

Lindl, J.D. (1995). *Phys. Plasmas* **2**, 3933.

Meyer-ter-Vehn, J. (1982). *Nucl. Fusion* **22**, 561.

Tabak, M., Hammer, J., Glinsky, M.E., Kruer, W.L., Wilks, S.C., Woodworth, J., Campbell, E.M. & Perry, M.D. (1994). *Phys. Plasmas* **1**, 1626.

Wilks, S.C. (1993). *Phys. Fluids B* **5**, 2603.

https://doi.org/10.1017/S0263034601191275 Published online by Cambridge University Press